World Academy of Science, Engineering and Technology
International Journal of Biomedical and Biological Engineering
Vol:16, No:10, 2022

Remote Vital Signs Monitoring in Neonatal Intensive Care Unit Using a Digital Camera

Fatema-Tuz-Zohra Khanam, Ali Al-Naji, Asanka G. Perera, Kim Gibson, Javaan Chahl

***Abstract*—**Conventional contact-based vital signs monitoring sensors such as pulse oximeters or electrocardiogram (ECG) may cause discomfort, skin damage, and infections, particularly in neonates with fragile, sensitive skin. Therefore, remote monitoring of the vital sign is desired in both clinical and non-clinical settings to overcome these issues. Camera-based vital signs monitoring is a recent technology for these applications with many positive attributes. However, there are still limited camera-based studies on neonates in a clinical setting. In this study, the heart rate (HR) and respiratory rate (RR) of eight infants at the Neonatal Intensive Care Unit (NICU) in Flinders Medical Centre were remotely monitored using a digital camera applying color and motion-based computational methods. The region-of-interest (ROI) was efficiently selected by incorporating an image decomposition method. Furthermore, spatial averaging, spectral analysis, band-pass filtering, and peak detection were also used to extract both HR and RR. The experimental results were validated with the ground truth data obtained from an ECG monitor and showed a strong correlation using the Pearson correlation coefficient (PCC) 0.9794 and 0.9412 for HR and RR, respectively. The root mean square errors (RMSE) between camera-based data and ECG data for HR and RR were 2.84 beats/min and 2.91 breaths/min, respectively. A Bland Altman analysis of the data also showed a close correlation between both data sets with a mean bias of 0.60 beats/min and 1 breath/min, and the lower and upper limit of agreement -4.9 to + 6.1 beats/min and -4.4 to +6.4 breaths/min for both HR and RR, respectively. Therefore, video camera imaging may replace conventional contact-based monitoring in NICU and has potential applications in other contexts such as home health monitoring.

***Keywords*—**Neonates, NICU, digital camera, heart rate, respiratory rate, image decomposition.

I. Introduction

VITAL signs, including RR, HR, heart rate variability (HRV), blood oxygen saturation (SpO2), temperature, blood pressure (BP) are important parameters to assess the condition of individuals health [1]-[3]. In NICU, vital signs of neonates, who are born prematurely or have health issues, are monitored continuously by various monitoring sensors, such as ECG, pulse oximeters, nasal thermocouples, piezoelectric transducers, and respiratory belt transducers [4]. These monitoring sensors are attached to the neonates with wires, straps, electrodes, or probes, which may cause painful stimuli, discomfort, skin irritation, and even skin damage when the adhesive sensors are removed as neonates have fragile, sensitive skin [5]. These complications can lead to injuries such as strangulation or entanglement, bacterial and fungal infection risk, and sleep disruption for the neonates [6]. Moreover, bonding of parent-infant, especially at the time of kangaroo mother care, is impaired due to obtrusiveness of the wires [7]. In recent years, non-contact remote vital sign monitoring techniques, including dopplers [8], [9], thermal/infrared imaging [10], [11] and video camera imaging [12]-[14], have been effective in solving the issues of contact vital sign monitoring approaches due to their unobtrusiveness and absence of physical contact.

Among non-contact techniques, video camera imaging is the most popular because of the high resolution and low cost of digital cameras [15]. The video camera imaging technology can be categorized into two main categories: motion-based methods and color-based methods. The first and second classes consider the cyclic motion of body areas such as head, chest, abdomen, and skin color variations caused by cardiorespiratory activity. Some researchers have considered motion-based methods [16]-[19] and others preferred the color-based methods [20]-[24] for monitoring vital signs remotely using advanced image and signal processing techniques. However, in all these studies, participants were adults; therefore, the investigation into the feasibility of remote monitoring of neonates in a clinical setting is limited.

Some studies have used video camera imaging technology for monitoring vital signs in the NICU. For instance, Scalise et al. [25] first proposed a non-contact HR monitoring system for newborns using a webcam in combination with a non-ambient green light. In this work, the ROI was selected manually. Independent component analysis (ICA) and power spectral density (PSD) were also used to extract HR. However, the infants were recorded only in supine positions in this work. The system was limited by short effective range, motion artifacts, light reflections, and unclear ROI due to occlusion of the ROI. Aarts et al. [26] first used ambient light to monitor the vital signs of 19 infants in a NICU and investigated different scenes with challenging conditions. In their work, for tracking the global motion of the infant, a manually chosen ROI was used as a template. Fourier analysis and a joint-time-frequency diagram (JFTD) were also considered. Nevertheless, the system was affected by infant motion and low ambient light.

Fatema-Tuz-Zohra Khanam is with the University of South Australia, Mawson Lakes Campus, SA 5095, Australia (e-mail: fatema-tuz-zohra.khanam@mymail.unisa.edu.au).

Ali Al-Naji is with the Electrical Engineering Technical College, Middle Technical University, Al Doura 10022, Baghdad, Iraq (e-mail: ali_al_naji@mtu.edu.iq)

Asanka G. Perera is with the University of New South Wales, Canberra ACT 2610, Australia.

Kim Gibson is with the University of South Australia, City East Campus, North Terrace, Adelaide, SA 5000, Australia (e-mail: Kim.Gibson@unisa.edu.au)

Javaan Chahl is with the University of South Australia, Mawson Lakes Campus, SA 5095, Australia (e-mail: Javaan.Chahl@unisa.edu.au)

A camera-based scheme was presented by Klaessens et al. [27] to monitor the RR and HR of seven neonates in NICU using RGB color magnification and infrared thermography (IRT). However, this system was also highly affected by motion. Another study by Gibson et al. [28] considered color magnification to measure HR and motion magnification to measure RR based on Eulerian video magnification (EVM). A method comparison study between the digital camera and the unit's ECG monitor was performed on 10 neonates in the NICU. However, the computational cost of EVM is high. Using two LWIR and three CMOS cameras, Paul et al. [29] performed another clinical study for monitoring the vital sign of 19 neonates. After a manual ROI selection, a kernelized correlation filter (KCF) was incorporated for tracking the ROI. The key issues pointed out by the authors were artefacts from motion, light sources, medical devices, and the detection and tracking of ROI to extract the signal.

An efficient and robust technique was proposed by Cobos-Torres et al. [30], considering multichannel analysis based on the least square method to lessen the effect of the moderate motion artefacts and changing light conditions. This work used a moving average filter, two narrowband filters, and a short-time Fourier transform (STFT). It was reported that, the proposed system needed 75% less CPU usage than ICA. Chen et al. [31] introduced another robust HR monitoring framework by resolving motion artifact challenges and considered nine hospitalized neonates. However, this study was conducted in a personal area with no noisy hospital environment and an unchanged lighting environment.

A study by Mestha et al. [32] introduced a continuous HR monitoring system where they recorded videos of eight newborns for 30 minutes each using a webcam. Another continuous monitoring scheme was presented by Villarroel et al. [33], where two neonates were monitored for 40 hours using a video camera. Nevertheless, this approach was constrained to unclear ROI, illumination variation, and subject movement. However, the ROI was selected manually in all the above-discussed studies.

To address some of these challenges, this paper aims to monitor the vital signs of neonates in NICU using a digital camera in normal neonatal scenarios that have affected previous results. Rather than selecting ROI manually, we have designed an efficient ROI selection method based on image decomposition. The main contributions of this study are as follows:

- Both HR and RR of neonates in NICU were remotely monitored using video camera imaging technology.
- Both color and motion-based methods have been used to measure HR and RR, respectively, which helps to measure RR even if the infant is covered with linen (i.e., ROI is unclear).
- An efficient ROI selection algorithm was introduced using image decomposition.
- A close correlation and small error rate between the measured data and ECG data demonstrated that video camera imaging technique may replace conventional contact-based monitoring in NICU and has potential applications in other areas such as remote home health monitoring.

Methods and materials, with study design, experimental set up for data collection in the NICU, and the system framework are explained in Section II. Then, the experimental results are represented and discussed in Section III. Lastly, the conclusion with the key findings, limitations, and future research directions are depicted in Section IV.

II. Methods and Materials

A. Study Design

A single-center cross-sectional experimental study was performed at Flinders Medical Centre NICU, a tertiary neonatal provision in Adelaide, South Australia. This study was approved by the Southern Adelaide Local Network Research Committee (HREC/17/SAC/340; SSA/17/SAC/341) and the University of South Australia Human Research Ethics Committee (Protocol number 0000034901). Prior to filming, the experimental procedure was thoroughly explained to the guardian of neonates and a written consent was also obtained from them.

We filmed eight neonates who were monitored using the regular ECG monitor of the unit. Seven neonates were preterm (gestational age was less than 37 weeks), and one neonate was greater than 37 weeks. Neonates who had abnormalities that may make them distinguishable in publications or who were not monitored by ECG or who were expected to be discharged during data collection were excluded in this study.

In this work, ECG was considered as the reference for validation purposes for all neonates. For extracting HR and RR, the difference in electrical impedance and the chest wall movement is measured by the impedance lead of the ECG, respectively. ECG is constrained to patient movement and cardiac activity [34]; however, it was used for validation purpose to avoid interruption to the neonates.

B. Experimental Set-Up

This study used two digital cameras mounted on tripods to record videos, as depicted in Fig. 1. A Nikon D610 with resolution 1920×1080 and frame rate 30 fps was used to capture the video of the neonate. On the other hand, a Nikon D5300 was used to record the video of the ECG monitor. Videos from each camera started at the same time, for synchronizing datasets from the proposed method and the ECG monitor. The videos were saved in .MOV format. The distance between camera and subject was 1-2 meters. Ten-minute-long videos of each neonate were recorded. For the experiment, 10 second videos were considered when neonates remained stable, i.e., not moving. For each neonate, five samples were considered for data analysis.

C. System Framework

As shown in Fig. 2, the overall system includes numerous techniques: video decomposition into tiles, ROI selection, spatial averaging, spectral analysis, band-pass filtering, and peak detection.

Fig. 1 Experimental setup for data collection

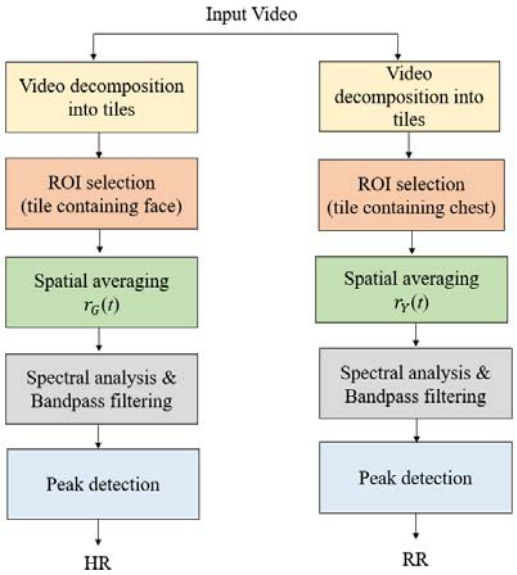

Fig. 2 System framework

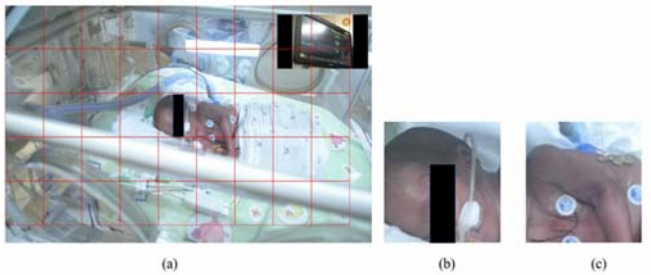

Fig. 3 Video decomposition and ROI selection: (a) Image decomposed into tiles, (b) Tile containing face considered as an ROI for HR, (c) Tile containing chest considered as an ROI for RR

a. Video Decomposition

The first frame of the raw video was first decomposed into tile images. To create a tile video from ROI, each frame was divided into small tiles corresponding to the grid in Fig. 3 (a). The tile size $d \times d$ was selected heuristically. Creating of tiles was started from the (1,1) image coordinate on the raw image frame. When the image width or height are not integer multiples of d, the tiles do not cover the whole raw image frame. In such cases, we consider only the area covered by the tiles on the raw image frame (i.e., the red grid in Fig. 3 (a) shows the selected tiles and each grid cell represents a tile video).

The total number of tiles is given by:

$$N_T = \lfloor W/d \rfloor \times \lfloor H/d \rfloor. \quad (1)$$

W and H are the width and height of the raw image frame.

Each ROI tile video was constructed with the same number of frames and at the same frame rate as the raw video.

b. ROI Selection

Each ROI was selected from the decomposed image. The tile which contained the face region was selected as ROI to calculate HR and the tile containing the chest region was chosen as ROI to calculate RR, as shown in Fig. 3. We repeated the same process for all frames.

In the standard manual ROI selection method, the face or chest area is selected by drawing a bounding box around it. The area covered by the bounding box is used to extract the vital signs. Here, instead of manual bounding boxes, we select the tiles where the ROI is located. This was done by visual inspection. The selected tiles for Fig. 3 (a) are shown in Figs. 3 (b) and (c). The main advantage of this ROI selection is we do not need to change ROI bounding boxes every time the baby changes pose. Normally, the baby moves only sideways, and therefore the face and chest areas always remain within the initially selected tiles. As the tile size is adjustable, we can set a safe tile size allowing the baby's movements. This visual tile selection can be replaced with a baby detection machine learning model. However, we found that this approach is difficult as (i) it is difficult to collect a sufficiently large dataset of babies, (ii) the available images contain complex equipment that occludes the view of the child, and (iii) higher numbers of fault detections were noticed with available human detectors when there were toys and baby like shapes on the bedsheet are present.

c. Spatial Averaging

In this study, color-based, and motion-based computational approaches were used for extracting raw cardiac and respiratory signals, respectively. Light absorbed by hemoglobin in blood is more than the adjacent tissue and causes a color variation in human skin. This color variation is not noticeable with naked eyes but can be revealed by a digital camera. The color variation reflects the blood volume variation in the microvascular tissue bed under the skin caused by changes in pulsatile blood flow during each cardiac cycle. Hence, using this principle, the cardiac signal can be measured. First, the green channel of RGB color space was chosen. Then, by calculating the average of the brightness pixels of the selected ROI, a raw cardiac signal was measured as depicted in (2). This was done to reduce camera noise enclosed in a single pixel and thus improve the signal to noise ratio.

$$r_G(t) = \frac{\sum_{i,j \in ROI} R(i,j,t)}{|ROI|} \quad (2)$$

where $R(i,j,t)$ represents the brightness pixel value at image

location (i,j) at a time (t), and $|ROI|$ is the size of the selected ROI. Compared to the red and blue channels the green channel has the strongest cardiac frequency band [20]. Therefore, the $r_G(t)$ signal was chosen to measure the cardiac signal.

During respiration, a difference in the movement of the thoracoabdominal wall is caused by inhalation and exhalation. In the recorded videos, spatial differences in intensity values reflect the difference in the movement of the thoracoabdominal wall caused by respiration. Therefore, the respiratory signal can be measured based on this principle. It is necessary to isolate the intensity information from the color information as the digital camera recorded the video in the RGB color space. Therefore, the RGB color space was converted to the YIQ color space using MATLAB built-in function, called 'rgb2ntsc'. First, the Y channel of the YIQ color space was chosen. Then, by taking the mean of the pixels' intensity within the selected ROI, the raw respiratory signal was extracted as follows:

$$r_Y(t) = \frac{\sum_{i,j \in ROI} R(i,j,t)}{|ROI|} \quad (3)$$

where $R(i,j,t)$ represents the intensity value of a pixel in Y channel at image location (i,j) at a time (t), and $|ROI|$ represents the size of the chosen ROI.

d. Spectral Analysis and Band-Pass Filtering

The raw time series cardiorespiratory signals were transformed from the time domain to the frequency domain based on spectral analysis technique using Fast Fourier Transform (FFT). Then, to acquire the frequency band of interest, two ideal band-pass filters were implemented at 1.5 Hz to 3 Hz corresponding to the pulse range (90–180 beats/min), as well as 0.3 Hz to 1.67 Hz, which corresponds to the breathing range (18–100 breaths/min). After that, the inverse FFT was implemented on the filtered signals to attain the time series cardiac and respiratory signals.

e. Peak Detection

The periodicity of peaks, peak locations, and the number of peaks of the attained signals were determined by using the peak detection method using the MATLAB built-in function 'findpeaks'. After identifying the peaks and their locations (locs), the total cycle length (C_T) between two peaks can be calculated using the equation:

$$C_T = \text{mean (diff (locs))}, \quad (4)$$

The number of peaks (p) can be found as:

$$p = \frac{t}{C_T} \quad (5)$$

where t signifies the length of video recording in seconds.

HR and RR per minute could be calculated using the equation:

$$C_M = \frac{60p}{t} \quad (6)$$

where C_M symbolizes the measured value.

III. Experimental Results

To implement the proposed algorithm and compute the statistical results, MATLAB 2020a was used. Fig. 3 shows the video decomposition and ROI selection process. As shown in Fig. 3 (a), the image with size 1920×1080 was divided into tiles with size 200×200. The total number of tiles was 45. Among 45 tiles, the 23rd number tile contained the face, which was considered as ROI for HR calculation (Fig. 3 (b)), and 24th number tile contained the chest and was chosen as ROI for RR calculation (Fig. 3 (c)). We repeated the same process for all frames.

The time series cardiac signal was obtained by calculating the mean of the pixel values over the selected ROI, as depicted in Fig. 4 (a). FFT, band-pass filtering and inverse FFT were implemented to achieve the filtered cardiac signal and shown in Fig. 4 (b). The HR was calculated by calculating the number of peaks from the filtered cardiac signal. Likewise, Figs. 5 (a) and (b) represent the raw respiratory signal and filtered respiratory signal, respectively. RR could also be calculated by calculating the number of peaks from the filtered respiratory signal.

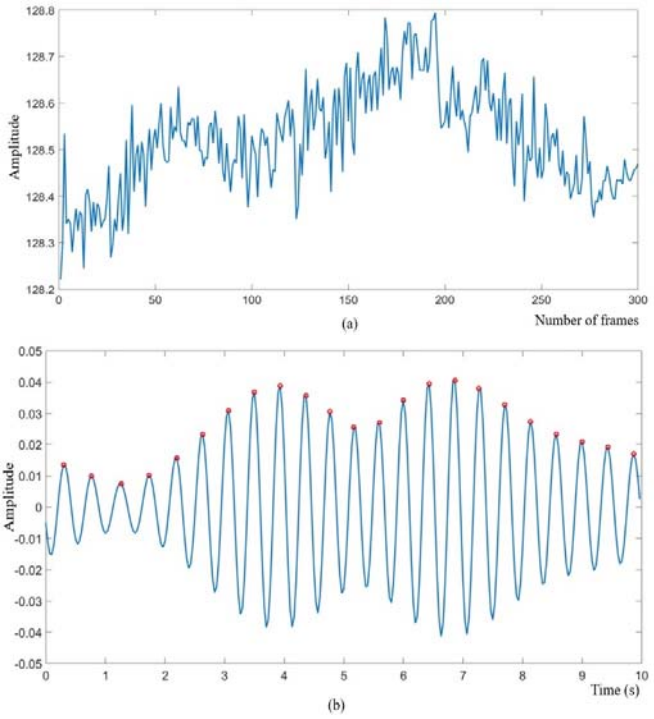

Fig. 4 Cardiac signal: (a) Raw cardiac signal, (b) filtered cardiac signal

Different statistical techniques, for example, the mean absolute error (MAE), RMSE, PCC, linear regression, and Bland Altman (BA) plot, were considered for the evaluation purpose. A total sample size of n = 40 was considered. Fig. 6 presents a correlation plot for HR, and Fig. 7 represents a BA plot for HR. A strong correlation between the ECG data and measured camera-based data with a PCC of 0.9794 can be observed in Fig. 6. It can be seen from Fig. 7 that the lower and

upper limits of agreements were -4.9 to + 6.1 beats/min, the mean bias was 0.6 beats/min, and the reproducibility coefficient (RPC) was 5.5 beats/min (3.7%). RMSE and MAE for HR were 2.84 beats/min and 2.18 beats/min, respectively.

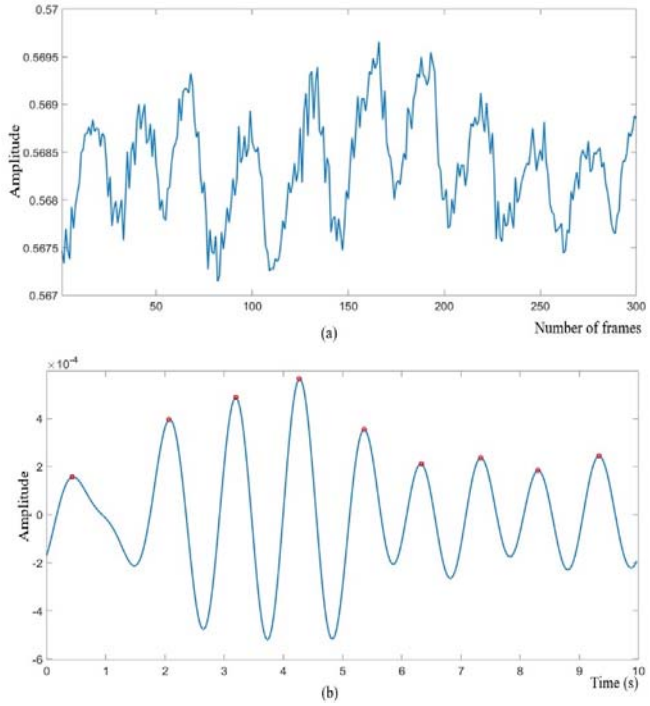

Fig. 5 Respiratory signal: (a) Raw respiratory signal, (b) filtered respiratory signal

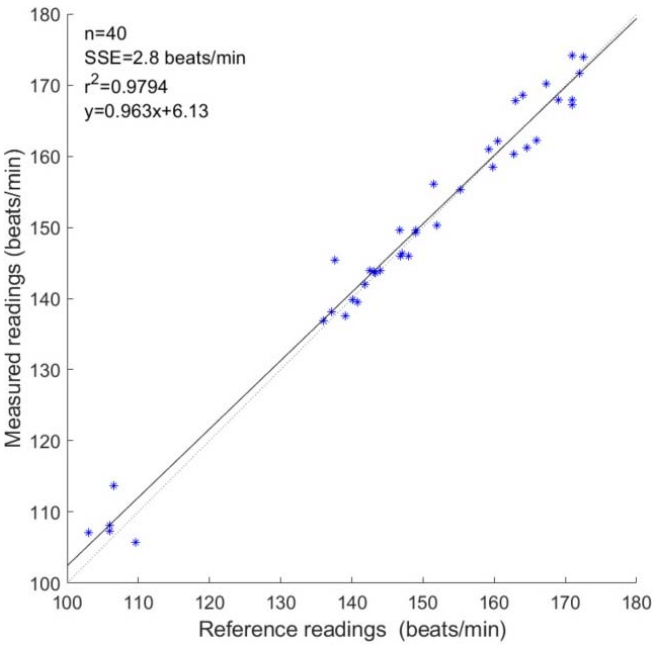

Fig. 6 Correlation plot for HR

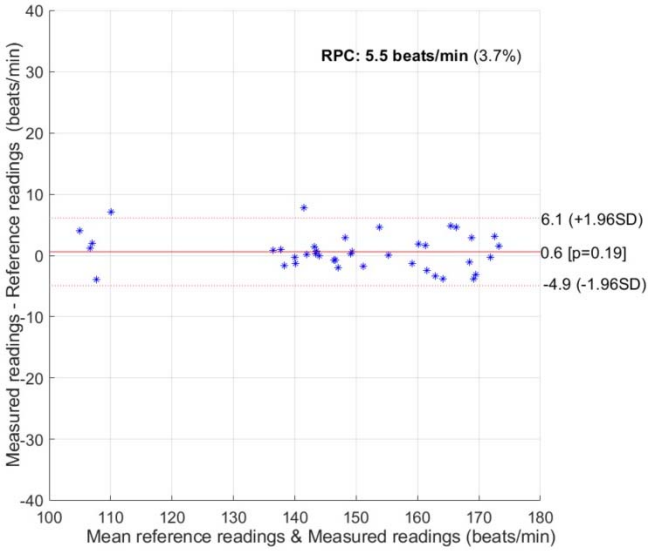

Fig. 7 BA plot for HR

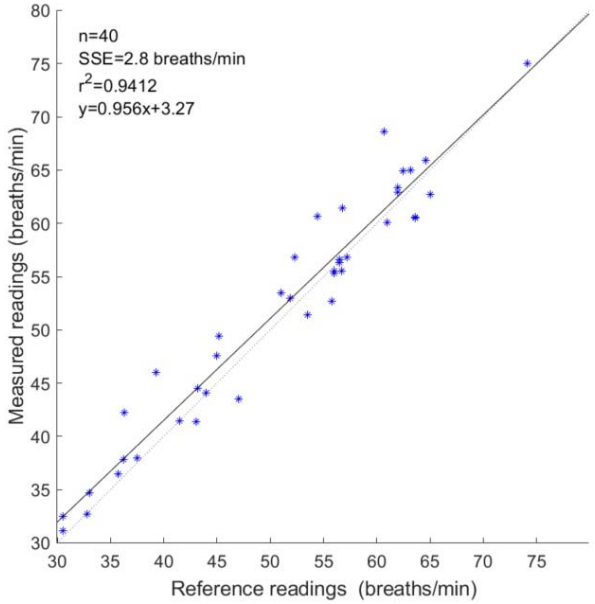

Fig. 8 Correlation plot for RR

Figs. 8 and 9 show a correlation plot and a BA plot for RR, respectively. A good correlation exists between the ECG data and measured camera-based data with a PCC of 0.9412 (Fig. 8). The BA plot in Fig. 9 represents RPC 5.4 breaths/min (11%), mean bias 1 breaths/min, and the lower and upper limit of agreement -4.4 to +6.4 breaths/min. RMSE was 2.91 breaths/min, and MAE was 2.17 breaths/min for RR.

It can be concluded that the proposed video camera imaging approach represented a good correlation with the reference system with a small error rate for both HR and RR.

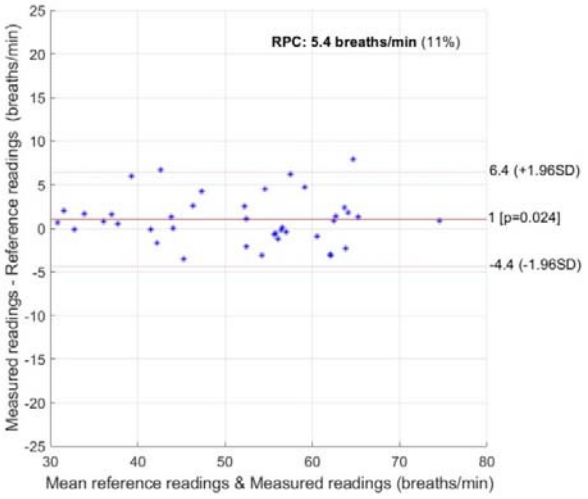

Fig. 9 BA plot for RR

IV. Conclusion

In this study, the HR and RR of eight infants in NICU were remotely monitored using a digital camera to overcome the limitation of conventional contact-based monitoring sensors. The ROI was efficiently selected incorporating an image decomposition method rather than using manual ROI selection. The experimental results demonstrated a strong correlation between proposed camera-based data and ECG data using the PCC 0.9794 and 0.9412 for HR and RR, respectively. The RMSE between both data sets for HR and RR were 2.84 beats/min and 2.91 breaths/min, respectively. A BA analysis of the data also showed a good correlation between both data sets for both HR and RR, respectively. As a result, it can be concluded that the video camera imaging technique might be applicable in the NICU in hospitals as well as representing a potential application in home health monitoring. Nevertheless, in this study, to calculate the cardiorespiratory signal, the videos were considered when infants remained still, and data from ECG were also stable. In the future, advanced signal process techniques will be needed to minimize the noise artifacts caused by subject movement, camera movement and illumination variations and more advanced image processing techniques will be required to select ROI automatically. Moreover, in this study, only eight infants were considered as participants; therefore, to make the system feasible for real-time application; more participants will need to be considered in the future.

Acknowledgment

The authors would like to thank the Government of South Australia and staff of the Flinders Medical Centre NICU for giving administrative access and support.

References

[1] X. Chen, J. Cheng, R. Song, Y. Liu, R. Ward, and Z. J. Wang, "Video-Based Heart Rate Measurement: Recent Advances and Future Prospects," *IEEE Transactions on Instrumentation and Measurement,* 2018.

[2] F.-T.-Z. Khanam, A. Al-Naji, and J. Chahl, "Remote Monitoring of Vital Signs in Diverse Non-Clinical and Clinical Scenarios Using Computer Vision Systems: A Review," *Applied Sciences,* vol. 9, no. 20, p. 4474, 2019.

[3] F.-T.-Z. Khanam *et al.*, "Noncontact Sensing of Contagion," *Journal of Imaging,* vol. 7, no. 2, p. 28, 2021.

[4] F. Zhao, M. Li, Y. Qian, and J. Z. Tsien, "Remote measurements of heart and respiration rates for telemedicine," *PloS one,* vol. 8, no. 10, p. e71384, 2013.

[5] M. M. Baharestani, "An overview of neonatal and pediatric wound care knowledge and considerations," *Ostomy/wound management,* vol. 53, no. 6, p. 34, 2007.

[6] J. M. Kuller, "Skin breakdown: risk factors, prevention, and treatment," *Newborn and Infant Nursing Reviews,* vol. 1, no. 1, pp. 35-42, 2001.

[7] R. G. Pineda *et al.*, "Alterations in brain structure and neurodevelopmental outcome in preterm infants hospitalized in different neonatal intensive care unit environments," *The Journal of pediatrics,* vol. 164, no. 1, pp. 52-60. e2, 2014.

[8] W. Lv, W. He, X. Lin, and J. Miao, "Non-Contact Monitoring of Human Vital Signs Using FMCW Millimeter Wave Radar in the 120 GHz Band," *Sensors,* vol. 21, no. 8, p. 2732, 2021.

[9] M. Mercuri, Y.-H. Liu, I. Lorato, T. Torfs, A. Bourdoux, and C. Van Hoof, "Frequency-tracking CW Doppler radar solving small-angle approximation and null point issues in non-contact vital signs monitoring," *IEEE transactions on biomedical circuits and systems,* vol. 11, no. 3, pp. 671-680, 2017.

[10] A. K. Abbas, K. Heiman, T. Orlikowsky, and S. Leonhardt, "Non-contact respiratory monitoring based on real-time IR-thermography," in *World Congress on Medical Physics and Biomedical Engineering, September 7-12, 2009, Munich, Germany*, 2009: Springer, pp. 1306-1309.

[11] S. Bennett, T. N. El Harake, R. Goubran, and F. Knoefel, "Adaptive Eulerian Video Processing of Thermal Video: An Experimental Analysis," *IEEE Transactions on Instrumentation and Measurement,* vol. 66, no. 10, pp. 2516-2524, 2017.

[12] A. Al-Naji and J. Chahl, "Contactless cardiac activity detection based on head motion magnification," *International Journal of Image and Graphics,* vol. 17, no. 01, p. 1750001, 2017.

[13] J. Cheng, X. Chen, L. Xu, and Z. J. Wang, "Illumination variation-resistant video-based heart rate measurement using joint blind source separation and ensemble empirical mode decomposition," *IEEE journal of biomedical and health informatics,* vol. 21, no. 5, pp. 1422-1433, 2017.

[14] F.-T.-Z. Khanam, A. G. Perera, A. Al-Naji, K. Gibson, and J. Chahl, "Non-contact automatic vital signs monitoring of infants in a neonatal intensive care unit based on neural networks," *Journal of Imaging,* vol. 7, no. 8, p. 122, 2021.

[15] A. Al-Naji, K. Gibson, S.-H. Lee, and J. Chahl, "Monitoring of cardiorespiratory signal: Principles of remote measurements and review of methods," *IEEE Access,* vol. 5, pp. 15776-15790, 2017.

[16] G. Balakrishnan, F. Durand, and J. Guttag, "Detecting pulse from head motions in video," in *Proceedings of the IEEE Conference on Computer Vision and Pattern Recognition*, 2013, pp. 3430-3437.

[17] A. Al-Naji and J. Chahl, "Detection of cardiopulmonary activity and related abnormal events using Microsoft Kinect sensor," *Sensors,* vol. 18, no. 3, p. 920, 2018.

[18] J.-P. Lomaliza and H. Park, "Detecting Pulse from Head Motions Using Smartphone Camera," in *International Conference on Advanced Engineering Theory and Applications*, 2016: Springer, pp. 243-251.

[19] A. Al-Naji and J. Chahl, "Remote respiratory monitoring system based on developing motion magnification technique," *Biomedical Signal Processing and Control,* vol. 29, pp. 1-10, 2016.

[20] W. Verkruysse, L. O. Svaasand, and J. S. Nelson, "Remote plethysmographic imaging using ambient light," *Optics express,* vol. 16, no. 26, pp. 21434-21445, 2008.

[21] M.-Z. Poh, D. J. McDuff, and R. W. Picard, "Non-contact, automated cardiac pulse measurements using video imaging and blind source separation," *Optics express,* vol. 18, no. 10, pp. 10762-10774, 2010.

[22] W. Wang, A. C. den Brinker, S. Stuijk, and G. de Haan, "Algorithmic principles of remote PPG," *IEEE Transactions on Biomedical Engineering,* vol. 64, no. 7, pp. 1479-1491, 2017.

[23] A. Al-Naji and J. Chahl, "Remote Optical Cardiopulmonary Signal Extraction with Noise Artifact Removal, Multiple Subject Detection & Long-Distance," *IEEE Access,* vol. 6, pp. 11573-11595, 2018.

[24] F. Bousefsaf, C. Maaoui, and A. Pruski, "Continuous wavelet filtering on webcam photoplethysmographic signals to remotely assess the instantaneous heart rate," *Biomedical Signal Processing and Control,* vol. 8, no. 6, pp. 568-574, 2013.

[25] L. Scalise, N. Bernacchia, I. Ercoli, and P. Marchionni, "Heart rate measurement in neonatal patients using a webcamera," in *2012 IEEE*

International Symposium on Medical Measurements and Applications Proceedings, 2012: IEEE, pp. 1-4.

[26] L. A. Aarts *et al.*, "Non-contact heart rate monitoring utilizing camera photoplethysmography in the neonatal intensive care unit—A pilot study," *Early human development,* vol. 89, no. 12, pp. 943-948, 2013.

[27] J. H. Klaessens, M. van den Born, A. van der Veen, J. Sikkens-van de Kraats, F. A. van den Dungen, and R. M. Verdaasdonk, "Development of a baby friendly non-contact method for measuring vital signs: first results of clinical measurements in an open incubator at a neonatal intensive care unit," in *Advanced Biomedical and Clinical Diagnostic Systems XII*, 2014, vol. 8935: International Society for Optics and Photonics, p. 89351P.

[28] K. Gibson *et al.*, "Non-contact heart and respiratory rate monitoring of preterm infants based on a computer vision system: a method comparison study," *Pediatric Research,* p. 1, 2019.

[29] M. Paul *et al.*, "Non-contact sensing of neonatal pulse rate using camera-based imaging: a clinical feasibility study," *Physiological Measurement,* vol. 41, no. 2, p. 024001, 2020.

[30] J.-C. Cobos-Torres, M. Abderrahim, and J. Martínez-Orgado, "Non-Contact, Simple Neonatal Monitoring by Photoplethysmography," *Sensors,* vol. 18, no. 12, p. 4362, 2018.

[31] Q. Chen *et al.*, "Camera-based heart rate estimation for hospitalized newborns in the presence of motion artifacts," *BioMedical Engineering OnLine,* vol. 20, no. 1, pp. 1-16, 2021.

[32] L. K. Mestha, S. Kyal, B. Xu, L. E. Lewis, and V. Kumar, "Towards continuous monitoring of pulse rate in neonatal intensive care unit with a webcam," in *2014 36th Annual International Conference of the IEEE Engineering in Medicine and Biology Society*, 2014: IEEE, pp. 3817-3820.

[33] M. Villarroel *et al.*, "Continuous non-contact vital sign monitoring in neonatal intensive care unit," *Healthcare technology letters,* vol. 1, no. 3, pp. 87-91, 2014.

[34] E. C. Eichenwald, "Apnea of prematurity," *Pediatrics,* vol. 137, no. 1, 2016.